Acta Crystallographica Section D
Biological Crystallography
ISSN 0907-4449

Crystallization and preliminary crystallographic data of a leucotoxin S component from *Staphylococcus aureus*

Valérie Guillet,[a] Daniel Keller,[b] Gilles Prévost[b] and Lionel Mourey[a]*

[a]Groupe de Biophysique Structurale, Département 'Mécanismes Moléculaires des Infections Mycobactériennes', IPBS–CNRS, 205 Route de Narbonne, 31077 Toulouse CEDEX, France, and [b]Laboratoire de Physiopathologie et d'Antibiologie des Infections Bactériennes Emergentes et Nosocomiales–EA 3432, Institut de Bactériologie de la Faculté de Médecine–Hôpitaux Universitaires de Strasbourg, 3 Rue Koeberlé, 67000 Strasbourg, France

Correspondence e-mail: lionel.mourey@ipbs.fr

Received 16 October 2003
Accepted 17 December 2003

Class S proteins of staphylococcal bicomponent pore-forming leucotoxins play an important role in membrane targetting and cell specificity. Wild-type and recombinant S components of the Panton–Valentine leucocidin (LukS-PV) were expressed in *Staphylococcus aureus* and *Escherichia coli*, respectively, and purified. Both proteins were crystallized in two crystal forms with Jeffamine M-600 as the precipitant at 285 K using the hanging-drop vapour-diffusion method and seeding techniques. Crystals belong to space group $P2$ (or $P2_1$) and $P4_1$ (or $P4_3$), with unit-cell parameters a = 72.3, b = 95.1, c = 108.1 Å, β = 106.4° and $a = b$ = 94.8, c = 306.2 Å, respectively. A full set of X-ray diffraction data was collected to 2.1 Å from a single tetragonal crystal of the wild-type protein at 100 K.

1. Introduction

Bicomponent leucotoxins belong to the family of staphylococcal pore-forming toxins rich in β-sheet structures (Menestrina *et al.*, 2001). These bipartite virulence factors are composed of class S proteins (32 kDa) that primarily bind to more-or-less specific membrane ligands (Gauduchon *et al.*, 2001) and allow the consecutive interaction of class F proteins (34 kDa). The oligomerization of these proteins results in prepores that sensitize mammalian cells to a series of activation pathways, and leads to the formation of β-barrel pores which are permeable to monovalent cations and which in turn disrupt cellular membranes (Prévost *et al.*, 2003).

To date, four loci encoding a leucotoxin entity have been characterized in *Staphylococcus aureus*. Three of them, encoding the Panton–Valentine (LukS-PV-LukF-PV), LukE-LukD and LukM-LukF′-PV leucocidins, are non-constant amongst bacterial isolates, but the strains producing the first two have been clearly associated with diseases such as furuncles, community pneumonia, post-antibiotic diarrhoea and impetigo (Prévost *et al.*, 2003). Class S proteins display 59–79% sequence identity, whereas proteins belonging to class F display 71–79% sequence identity. S and F proteins share only 20–30% identity when compared with each other or with the single-component staphylococcal α-haemolysin (α-toxin), the β-barrel pore-forming toxin prototype. The crystal structure of the fully assembled α-haemolysin, a detergent-solubilized heptamer, has been determined (Song *et al.*, 1996). Each protomer of the α-haemolysin heptamer is organized into three structural domains: the β-sandwich and the rim domains, which form the protein core, and the central 40-residue stem domain, which protrudes from this core as a β-hairpin that constitutes the building unit of the membrane-spanning 14-stranded β-barrel. The X-ray structures of the water-soluble monomers of two class F proteins have also been determined: HlgB (Olson *et al.*, 1999) and LukF-PV (Pédelacq *et al.*, 1999). The monomeric proteins contain a core structure very similar to that of an individual protomer of α-haemolysin. However, in contrast to the α-haemolysin protomer, their stem region forms a three-strand antiparallel β-sheet that packs against the β-sandwich domain. Other striking differences occur in the N-terminal region, which in these proteins participates in the β-sheet structure of the sandwich domain, whereas in α-haemolysin it extends from the core of the protomer to interact with a neighbouring subunit, contributing to the stability of the heptameric assembly.

The structures of the HlgB and LukF-PV monomers and of the α-haemolysin heptamer illustrate the molecular species involved in the first and last steps of pore formation, respectively. They provide useful models for understanding the general structure–function relationships in the β-barrel pore-forming toxin superfamily (Heuck *et al.*, 2001) and also provide some description of the mechanism of toxin assembly in *Staphylococcus* sp. (Olson *et al.*, 1999; Pédelacq *et al.*, 1999). However, no crystal structure is available for the S monomer nor for the assembled leucotoxin hetero-oligomer. The structure determination of an S

monomer is important owing to its particular role in membrane targetting. This is especially the case for LukS-PV, which is assumed to interact with a membrane receptor and leads to a Panton–Valentine leucocidin that displays a narrow cell specificity. Such a structure would also provide an insight into the protein–protein interactions that sustain the final bipartite molecular architecture. We have recently succeeded in crystallizing wild-type (284 residues, 32.3 kDa) and recombinant (292 residues, 33.1 kDa) LukS-PV and we report here our preliminary crystallographic studies of these proteins.

2. Materials and methods

2.1. Expression and purification of wild-type and recombinant LukS-PV

The reference *S. aureus* ATCC 49775 was grown at 310 K for 16 h with vigorous shaking in 12 Erlenmeyer flasks containing 170 ml YCP medium (Prévost *et al.*, 1995). Bacteria were discarded by centrifugation and filtration with a 0.45 µm filter (Millipore, Paris, France) and the protein content of the culture supernatant was precipitated using 80% ammonium sulfate (277 K, 16 h). The precipitated materials were harvested by centrifugation at 20 000*g* (20 min), resuspended in 50 m*M* sodium phosphate pH 7.0 (buffer *A*) and applied to an SP Sepharose Fast Flow column (Amersham Biosciences) equilibrated with buffer *A*. Proteins were eluted with a discontinuous gradient of sodium chloride. Fractions eluted at 0.5 *M* sodium chloride, which contained proteins immunoreactive to a rabbit polyclonal anti-LukS-PV antibody, were dialyzed against buffer *A* and supplemented further with ammonium sulfate to a final concentration of 1.5 *M*. The protein solution was then loaded onto an Alkyl-Superose column (Amersham Biosciences) equilibrated with 1.5 *M* ammonium sulfate in buffer *A* and eluted with a linear gradient of ammonium sulfate. The immunoreactive material obtained at about 0.8 *M* ammonium sulfate was dialyzed against 50 m*M* sodium chloride in buffer *A* and subjected to cation-exchange chromatography on a MonoS column (Amersham Biosciences) equilibrated with the same buffer and eluted with a linear gradient of 50–300 m*M* sodium chloride. The purified LukS-PV eluted at 170 m*M* sodium chloride. The protein was filtered using a 0.22 µm Millipore filter, concentrated to 1.5 mg ml^{-1} and stored at 277 K.

For production of the recombinant protein, the open reading frame of *lukS-PV* corresponding to the secreted LukS-PV was cloned as a glutathione *S*-transferase (GST) fusion protein into the *Eco*RI restriction site of the expression plasmid pGEX-6P-1 (Amersham Biosciences) and expressed in *Escherichia coli* (BL21) cells. Cloning, expression and purification of recombinant LukS-PV in 50 m*M* HEPES pH 7.5, 50 m*M* sodium chloride were as previously described (Baba Moussa *et al.*, 1999). A homogenous fraction of LukS-PV was finally obtained by further purification on a MonoS column using a linear gradient of 0.05–1.0 *M* sodium chloride in the above buffer. The protein was filtered using a 0.22 µm Millipore filter, concentrated to 2.4 mg ml^{-1} and stored at 277 K. The recombinant but fully functional protein contained eight additional residues (Gly-Pro-Leu-Gly-Ser-Pro-Glu-Phe) and will therefore be referred to as LukS+8-PV.

2.2. Crystallization and X-ray data collection and processing

All experiments were carried out using freshly prepared LukS-PV and LukS+8-PV proteins that had never been frozen. Dynamic light-scattering (DLS) experiments were performed prior to crystallization attempts. Scattered intensities were recorded at 293 K using a DynaPro-MS/X molecular-sizing instrument equipped with a microsampler (Protein Solutions). The experiments were conducted at several pH values in the range 6.0–8.0 and reasonable particle size and monodispersity were only obtained in the presence of a minimal ionic strength.

Crystallization was performed at 285 K by vapour equilibration using the hanging-drop method. The proteins were concentrated to 20–25 mg ml^{-1} in 50 m*M* MES–NaOH pH 6.0, 50 m*M* sodium chloride. Drops were prepared by mixing equal volumes of protein and reservoir solutions; reservoir volumes of 500 µl were used. Structure Screens 1 and 2 (Molecular Dimensions) based on previously crystallized proteins (Jancarik & Kim, 1991; Cudney *et al.*, 1994) were used for initial screening. The crystallization condition that initially led to crystalline material was observed with the wild-type protein: thin stacked plates unsuitable for diffraction studies appeared within a few days in the presence of Jeffamine M-600 as a precipitating agent. Further systematic screening of pH and precipitating agent concentration around these conditions led to thin rod-shaped crystals of LukS+8-PV that appeared in 20% Jeffamine M-600, 100 m*M* MES–NaOH pH 6.5. Microseeding and macroseeding techniques, including cross-seeding, were then used to grow crystals of both proteins pre-equilibrated at different pH values and Jeffamine M-600 concentrations. Rod-shaped crystals of wild-type LukS-PV were produced in this way and a further crystal form was also obtained for wild-type and recombinant protein: bipyramidal monocrystals were grown in 30% Jeffamine M-600, 0.1 *M* Tris–HCl at pH values ranging from 8.0 to 8.9. This crystal form was never obtained by spontaneous nucleation.

For cryocooling, all crystals were directly transferred into a stream of nitrogen gas at 100 K and stored in liquid nitrogen if necessary. The various crystal forms were evaluated in-house at 285 and 100 K using a Rigaku RU300 rotating-anode source operating at 50 kV and 90 mA and an R-AXIS IIc image-plate area detector. A native data set was collected from a single bipyramidal crystal of the wild-type protein at beamline ID14-1 of the European Synchrotron

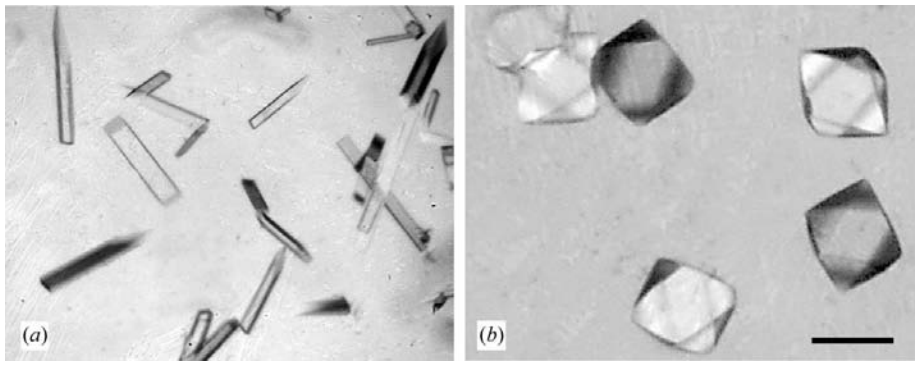

Figure 1
Crystals of LukS-PV from *S. aureus*. (*a*) Rod-shaped monoclinic crystals of the recombinant protein. (*b*) Bipyramidal tetragonal crystals of the wild-type protein. The two photomicrographs are displayed using the same scale; the scale bar corresponds to 0.2 mm.

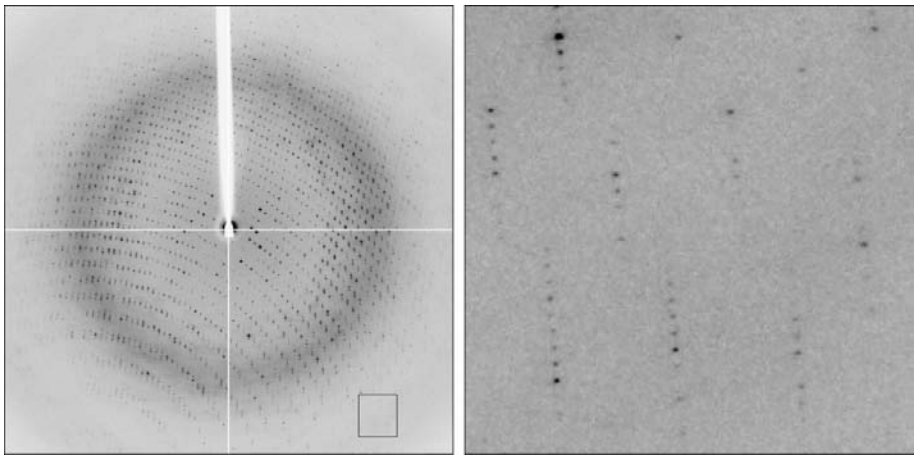

Figure 2
X-ray diffraction pattern from a tetragonal crystal of wild-type LukS-PV collected at ID14-1 (ESRF). Exposure time, 3 × 5 s; crystal-to-detector distance, 230 mm; oscillation angle, 1.0°. An ADSC Q4R CCD detector was used to record the image. The frame edge in the close-up view (right panel) is at 2.1 Å resolution.

Table 1
Data-collection statistics.

Values in parentheses correspond to the highest resolution shell.

Space group	$P4_1$ or $P4_3$
Unit-cell parameters (Å)	$a = b = 94.8$, $c = 306.2$
Resolution range (Å)	35.0–2.1 (2.21–2.10)
No. measured reflections	964279
No. unique reflections	153093
Redundancy	6.3
Completeness (%)	97.8 (87.0)
R_{sym} (%)	5.4 (33.5)
Mean $I/\sigma(I)$	8.2 (2.2)

Radiation Facility (ESRF, Grenoble, France). Data processing and scaling were performed using *MOSFLM* (Leslie, 1992) and *SCALA* (Collaborative Computational Project, Number 4, 1994). The crystal data were used to calculate a self-rotation function using *MOLREP* (Vagin & Teplyakov, 1997) and a self-Patterson map using *FFT* (Collaborative Computational Project, Number 4, 1994).

3. Results and discussion

We have initiated a process of crystal structure determination of a staphylococcal bicomponent leucotoxin class S protein that mediates cellular specificity. Although several proteins from various leucotoxins were expressed, purified and investigated for crystallization, only Panton–Valentine leucocidin class S protein was crystallized. Wild-type (LukS-PV) and recombinant (LukS+8-PV) proteins were purified to homogeneity as judged from SDS–PAGE analysis. DLS studies indicated both proteins to be very sensitive to ionic strength. Monodisperse solutions were obtained in 50 m*M* MES–NaOH pH 6.0, 50 m*M* sodium chloride; the absence of salt or the use of protein buffer at pH 8.0 induced the formation of protein aggregates (data not shown).

Crystals were grown *ab initio* and using seeding techniques. Two crystal forms were obtained that could be easily distinguished owing to their crystal habits (rod-shaped and bipyramidal; Fig. 1). The best crystals of LukS+8-PV appeared as thin rods of maximum dimensions 0.2 × 0.04 × 0.04 mm. They belong to the monoclinic space group $P2$ (or $P2_1$), with unit-cell parameters $a = 72.3$, $b = 95.1$, $c = 108.1$ Å, $\beta = 106.4°$. The best crystals of LukS-PV appeared as bipyramids and belong to the tetragonal space group $P4_1$ (or its enantiomorph $P4_3$), with unit-cell parameters $a = b = 94.8$, $c = 306.2$ Å. It is noteworthy that tetragonal crystals were also obtained for LukS+8-PV. However, the highest resolution was systematically achieved using tetragonal crystals of the wild-type protein, whereas crystals of the recombinant protein displayed anisotropic diffraction patterns.

A complete native data set was collected from a single tetragonal crystal of LukS-PV (0.2 × 0.2 × 0.2 mm). The images clearly show diffraction to 2.1 Å (Fig. 2). Statistics of the X-ray data collection and processing are given in Table 1. The number of molecules in the crystallographic asymmetric unit was estimated using the Matthews probability calculator, which includes resolution as additional information (Kantardjieff & Rupp, 2003). The highest probabilities were obtained with eight to ten molecules in the asymmetric unit, giving Matthews coefficients (V_M values; Matthews, 1968) and solvent contents ranging from 2.7 to 2.1 Å^3 Da^{-1} and from 54 to 42%, respectively. The tendency of the protein to aggregation and the large number of copies in the asymmetric unit being related to the formation of a high-order quaternary structure reflecting a functional oligomer is unlikely for two reasons. Firstly, the leucocidin F and S components have never been reported to form homo-oligomeric structures in solution and the formation of hetero-oligomers requires cellular or synthetic membranes (Colin *et al.*, 1994; Meunier *et al.*, 1997). Secondly, the self-rotation function and the self-Patterson map indicate that the molecules in the asymmetric unit are related by a combination of non-crystallographic twofold axes and a translation vector. No molecular axis of higher symmetry could be identified, suggesting that the number of LukS-PV molecules in the asymmetric unit is an artifact of crystal packing. A full structure determination by the molecular-replacement method using the coordinates of LukF-PV, the Panton–Valentine leucocidin F component, is in progress.

We thank Françoise Viala for her help in preparing the figures. This work was supported by a grant (EA 3432 to GP) from the Direction de la Recherche et des Etudes Doctorales, France.

References

Baba Moussa, L., Werner, S., Colin, D. A., Mourey, L., Pédelacq, J. D., Samama, J. P., Sanni, A., Monteil, H. & Prévost, G. (1999). *FEBS Lett.* **461**, 280–286.
Colin, D. A., Mazurier, I., Sire, S. & Finck-Barbançon, V. (1994). *Infect. Immun.* **62**, 3184–3188.
Collaborative Computational Project, Number 4 (1994). *Acta Cryst.* D**50**, 760–763.
Cudney, B., Patel, S., Weisgraber, K., Newhouse, Y. & McPherson, A. (1994). *Acta Cryst.* D**50**, 414–423.
Gauduchon, V., Werner, S., Prévost, G., Monteil, H. & Colin, D. A. (2001). *Infect. Immun.* **69**, 2390–2395.
Heuck, A. P., Tweten, R. K. & Johnson, A. E. (2001). *Biochemistry*, **40**, 9065–9073.
Jancarik, J. & Kim, S.-H. (1991). *J. Appl. Cryst.* **24**, 409–411.
Kantardjieff, K. A. & Rupp, B. (2003). *Protein Sci.* **12**, 1865–1871.
Leslie, A. G. W. (1992). *Jnt CCP4/ESF–EACMB Newsl. Protein Crystallogr.* **26**, 27–33.
Matthews, B. W. (1968). *J. Mol. Biol.* **33**, 491–497.
Menestrina, G., Dalla Serra, M. & Prévost, G. (2001). *Toxicon*, **39**, 1661–1672.
Meunier, O., Ferreras, M., Supersac, G., Hoeper, F., Baba Moussa, L., Monteil, H., Colin, D. A., Menestrina, G. & Prévost, G. (1997). *Biochim. Biophys. Acta*, **1326**, 275–289.
Olson, R., Nariya, H., Yokota, K., Kamio, Y. & Gouaux, E. (1999). *Nature Struct. Biol.* **6**, 134–140.

Pédelacq, J. D., Maveyraud, L., Prévost, G., Baba Moussa, L., Gonzales, A., Courcelle, E., Shepard, W., Monteil, H., Samama, J. P. & Mourey, L. (1999). *Structure*, **7**, 277–287.

Prévost, G., Cribier, B., Couppié, P., Petiau, P., Supersac, G., Finck-Barbançon, V., Monteil, H. & Piémont, Y. (1995). *Infect. Immun.* **63**, 4121–4129.

Prévost, G., Menestrina, G., Colin, D. A., Werner, S., Bronner, S., Dalla Serra, M., Baba Moussa, L., Coraiola, M., Gravet, A. & Monteil, H. (2003). *Pore-Forming Peptides and Protein Toxins*, edited by G. Menestrina, M. Dalla Serra & P. Lazarovici, pp 3–26. London: Taylor & Francis.

Song, L., Hobaugh, M. R., Shustak, C., Cheley, S., Bayley, H. & Gouaux, J. E. (1996). *Science*, **274**, 1859–1866.

Vagin, A. & Teplyakov, A. (1997). *J. Appl. Cryst.* **30**, 1022–1025.